Chemical Science

ROYAL SOCIETY OF CHEMISTRY

EDGE ARTICLE

View Article Online
View Journal | View Issue

Cite this: *Chem. Sci.*, 2023, **14**, 5802

All publication charges for this article have been paid for by the Royal Society of Chemistry

Received 27th February 2023
Accepted 19th April 2023

DOI: 10.1039/d3sc01074k

rsc.li/chemical-science

Quantum chain amplification in nanocrystalline Dewar benzenes by intramolecular sensitization†

Edris Rivera, Indrajit Paul, Javier Fajardo, Jr and Miguel A. Garcia-Garibay *

Quantum chain reactions are characterized by the formation of several photoproducts per photon absorbed (Φ_{QC} > 1) and constitute a promising signal amplification mechanism. The triplet-sensitized isomerization of Dewar benzene is known to undergo quantum chain reactions characterized by an adiabatic valence-bond isomerization to the excited state of Hückel benzene, which is able to transfer its triplet energy to a new ground state Dewar benzene that reacts to continue the chain. Given that diffusion-mediated energy transfer is the chain-limiting event in solution, we demonstrate here that reactions in crystals are significantly more efficient by taking advantage of energy transfer by a presumed exciton delocalization mechanism. Using Dewar benzenes with covalently attached, high energy triplet sensitizers we have demonstrated the efficiency of the solid state by the amplification of a quantum yield of *ca.* $\Phi_{QC} \approx 76$ in acetonitrile solution to as much as *ca.* $\Phi_{QC} \approx 100$–120 in submicron size specimens prepared by the re-precipitation method, and up to *ca.* $\Phi_{QC} \approx 300$ with microcrystalline powders suspended in water.

Introduction

Most organic photochemical processes involve the excitation of a single molecule followed by return to the ground state by releasing heat, emitting a single photon, transferring its energy to another molecule, or undergoing a reaction to give a primary photoproduct.[1] Exceptions from this norm include nonlinear photochemical processes involving a non-identical number of photochemical events and photons absorbed. Such systems can be utilized for signal amplification devices, catalysis, and solar cells.[2–5] Examples include coherent and stepwise two photon absorption,[6,7] fusion of two or more low energy photons to generate one high-energy excited state by triplet–triplet annihilation,[8] and the fission of a single excitation generated with a high-energy photon that results in two excited states, each with half the energy of the original.[9,10] An equally interesting, but significantly less explored process, occurs when a single photon leads to many chemical events in a "quantum chain reaction".[11] Quantum chain reactions start by formation of an excited state (step 1, Scheme 1) and are followed by a relatively uncommon propagation step involving an adiabatic photochemical reaction where the photoproduct is formed in the excited state (step 2, Scheme 1).[12–15] This is followed by energy transfer to a new ground-state reactant that prolongs the chain (step 3, Scheme 1). Chain termination occurs when either the excited-state product (P*) or reactant (R*) undergo thermal or radiative decay (step 4 and/or step 5, Scheme 1).

Despite the promise offered by chemical systems leading to multiple events per photon absorbed, quantum chain reactions are limited both by the small number of adiabatic reactions known at this time and the lack of convenient strategies to optimize the energy transfer step.[16–32] In this regard, singlet state quantum chains are severely limited by the short lifetimes of the excited photoproducts, which make energy transfer by diffusion-mediated mechanisms unfavourable. In fact, adiabatic reactions that take place in the singlet state are commonly established by detecting the fluorescence[33,34] or transient absorption of the excited photoproduct, rather than by observation of a quantum yield of product formation that is greater than one, which is the key signature of a quantum chain. We

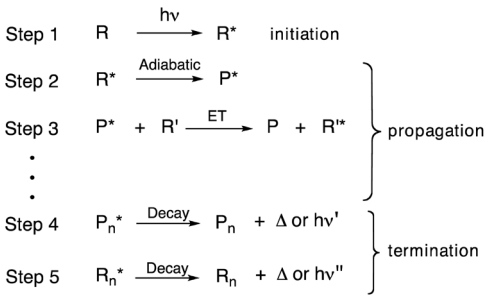

Scheme 1 Initiation, propagation and termination steps of a quantum chain reaction.

Department of Chemistry and Biochemistry, University of California, Los Angeles, CA 90095-1560, USA. E-mail: mgg@chem.ucla.edu

† Electronic supplementary information (ESI) available: Synthetic procedures and analytical data, nanocrystal characterization and photochemical protocols. CCDC 2084271. For ESI and crystallographic data in CIF or other electronic format see DOI: https://doi.org/10.1039/d3sc01074k

recently proposed that an effective way to circumvent this limitation is by carrying out quantum chain reactions in crystalline solids,[35,36] where energy transfer can occur by an ultrafast exciton delocalization mechanism.[37–41] We showed that the adiabatic decarbonylation of diphenylcyclopropenone to diphenyl acetylene could not enter a quantum chain process in solution despite having an adiabatic quantum yield $\Phi_{AR} = 1$ because there is no time for diffusion-mediated energy transfer within the *ca.* 8 ps lifetime of the excited photoproduct.[35,36,42] By contrast, quantum chain reactions with quantum yields up to $\Phi_{QC} = 3.3$ could be measured in aqueous nanocrystalline suspensions of diphenylcyclopropenone,[35,36] where energy transfer is mediated by a rapid exciton delocalization mechanism.[42] Efficient quantum chains ($\Phi_{QC} \gg 1$) require adiabatic reactions with high quantum efficiencies ($\Phi_{AR} \approx 1$) and are limited by the number of energy transfer steps, n, as shown in eqn (1)–(3),[36]

$$\Phi_{QC} = (\Phi_{AR})^1 + (\Phi_{AR})^2 + (\Phi_{AR})^3 + \ldots (\Phi_{AR})^n \quad (1)$$

$$\Phi_{AR} = k_{AR}/[k_{AR} + k_{R\text{-}dec}] \quad (2)$$

$$n = k_{ET}/k_{P\text{-}dec} \quad (3)$$

It should be noted that efficient adiabatic reactions ($\Phi_{AR} \approx 1$) require reaction rates that are much greater than that of the decay of the excited reactant by all other pathways ($k_{AR} \gg k_{R\text{-}dec}$). The maximum value n in eqn (1) is determined by the relative rates of energy transfer from the excited photoproduct (k_{ET}) in relation to its rate of decay ($k_{P\text{-}dec}$).[36]

Based on the above analysis, one may expect that triplet quantum chain reactions carried out in crystalline solids have the potential of reaching very high Φ_{QC} values by taking advantage of energy transfer by triplet exciton hopping, which is known to approach the picosecond time scale.[37–41,43] Assuming ideal adiabatic reactions with $\Phi_{AR} \approx 1$, the theoretical limit for a triplet quantum chain is given by the value of n in eqn (1), as defined in eqn (3). Based on a general approximation, one may expect $n = k_{ET}/k_{P\text{-}dec}$ to take values as large as 10^9 if triplet excitons were to have jumping rates of *ca.* $k_{ET} \approx 10^{12}$ s^{-1} and triplet lifetimes (τ_T) were to extend into the millisecond time scales ($\tau_T = 1/k_{dec} \approx 10^{-3}$ s).

As a first test of this hypothesis, we explore here the quantum chain reaction of crystalline Dewar benzene to Hückel benzene. Early studies by Turro[44] established a concentration-dependent quantum chain reaction that reaches a limiting experimental value of *ca.* $\Phi_{QC} = 0.5$ but extrapolates to $\Phi_{QC} \approx 10$ at infinite Dewar benzene concentration. It was shown that triplet energy sensitizers with $E_T > 63$ kcal mol^{-1} are required for efficient energy transfer, indicating an experimental upper limit for the triplet excitation energy of Dewar benzene.[44] More recently, using a Dewar benzene 3,4,5,6-tetramethyl-1,2-diester derivative (**DB-CO$_2$Me**, Scheme 2), Merkel *et al.* reported quantum yields as high as $\Phi_{QC} = 120$ in ethyl acetate,[45] and Ferrar *et al.* showed the feasibility of quantum chain reactions in polymer matrices upon the addition of external sensitizers and co-sensitizers.[46] In the latter example, reactions were carried out with reactant,

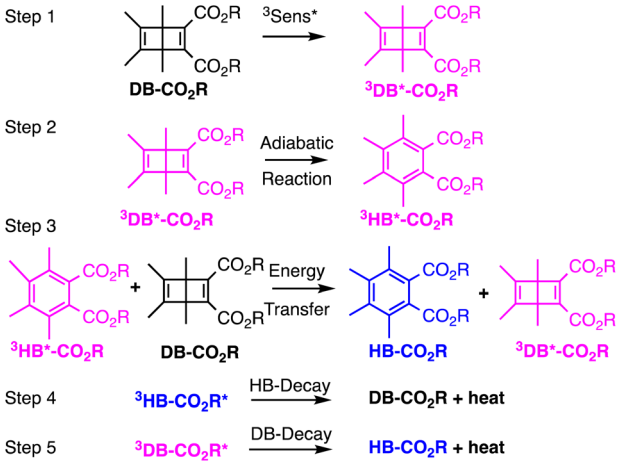

Scheme 2 Steps for the triplet sensitized quantum chain reaction of Dewar benzenes.

sensitizer and co-sensitizer randomly dispersed in the polymer matrix, such that a distribution of donor and acceptor distances can lead to a range of energy transfer efficiencies that affect both sensitization and chain propagation steps. By contrast, Dewar benzene molecules in crystals have the close proximity required for efficient energy transfer by an exciton delocalization mechanism, especially if the reactant is equipped with an intramolecular sensitizer. A simple solution to this problem is to substitute the dicarboxymethyl groups in **DB-CO$_2$Me** for 4-hydroxy-benzophenones in **DB-CO$_2$BPh** so that triplet sensitization can occur intramolecularly. It is well known that electronic excitation of the benzophenone chromophore leads to intersystem crossing and efficient formation of the triplet n, π^* excited state within a few picoseconds. Thus, the original excited state is localized on the benzophenone part of the bichromophoric compound (**DB-CO$_2$-^{3}BPh***, not shown in Scheme 2) and is followed by intramolecular energy transfer to the covalently attached Dewar benzene moiety **^{3}DB*-CO$_2$BPh**, which initiates the quantum chain (step 1). An adiabatic triplet state reaction forms the triplet excited state of the Hückel benzene photoproduct, **^{3}HB*-CO$_2$BPh** step 2, which acts as the quantum chain carrier. In step 3, the triplet photoproduct **^{3}HB*-CO$_2$BPh** should be well suited in crystals to transfer energy to a neighboring ground-state Dewar benzene **DB-CO$_2$BPh** to propagate the chain. While chain termination is expected to occur *via* steps 4 or 5 when either excited state decays back to the ground state manifold, step 5 is accounted for in the quantum yield of the adiabatic reaction, so that the chain length given by the value of n depends on the relative rates of step 3 and 4. As described below, we were able to demonstrate a concentration-dependent quantum chain in solution with modest values ranging from *ca.* $\Phi_{QC} \approx 2.5$–76 for reactant concentrations ranging from 5–50 mM. By contrast, quantum chain reactions carried out with samples prepared by the re-precipitation method led to average quantum chain values of *ca.* $\Phi_{QC} \approx 100$, even though the samples were shown to be semi-crystalline. Notably, a qualitative comparison of the latter with

microcrystalline powders suspended in water showed an increase in quantum chain values up to *ca.* $\Phi_{QC} \approx 300$. Evidence for a fast adiabatic reaction was obtained by nanosecond laser flash photolysis experiments showing that a long-lived transient generated from the starting Dewar benzene **DB-CO$_2$BPh** is identical to the one generated from the Hückel benzene isomer, which corresponds to the chain carrier **^{3}HB*-CO$_2$BPh**.

Experimental section

Synthesis and characterization of Dewar benzenes

Samples of Dewar benzene derivatives used in this study were prepared by conventional synthetic procedures that are described in the ESI section.†

Laser flash photolysis detection of the quantum chain carrier

Nanosecond laser flash photolysis experiments with **DB-CO$_2$BPh** and **HB-CO$_2$BPh** were carried out using a Brilliant B Quantel Nd:YAG laser operating at 355 nm with a pulse width of *ca.* 8 ns as the excitation source. Samples were introduced to a mounted 1 cm quartz flow cell through a continuous one-pass flow system to ensure that only unreacted material was continuously sampled. Samples were sparged with argon for at least an hour prior to flowing into the flow cell and remained continuously sparged for the entire experiment. The characteristic triplet–triplet absorption of the benzophenone sensitizer was determined by measuring the triplet absorption and lifetime of 4-acetoxybenzopheone (**4-AcOBPh**).

Quantum chain reaction in solution

The quantum yields of product formation from **DB-CO$_2$BPh** ($\Phi_{HB\text{-}OBPh}$) were determined using the photodecarbonylation of dicumyl ketone (**DCK**) as a chemical actinometer.[49] The selection of **DCK** was based on its known quantum yield in solution and in the solid state,[49] with the latter measured in nanocrystalline suspensions.[50] Thus, photochemical excitation of **DCK** in benzene solution at $\lambda = 312$ nm leads to the consumption of starting material with a quantum yield of $\Phi_{DCK(soln)} = 0.41 \pm 0.04$. Similarly, photochemical reactions in the crystalline state using optically dense nanocrystalline suspensions proceed with the exclusive formation of dicumene (**DC**) with a quantum yield of $\Phi_{DC(cryst)} = 0.20 \pm 0.02$.[49]

Results and discussion

Samples of **DB-CO$_2$BPh** proved to be crystalline after purification. Melting with concomitant reaction to the valence-bond isomerized product **HB-CO$_2$BPh** was shown to occur at *ca.* 109 °C. Diffraction data from cubic prisms obtained by slow evaporation from diethyl ether were solved in the space group $P2_1/n$ with 4 molecules per unit cell. Molecules of **DB-CO$_2$BPh** crystallize with the Dewar benzene fragments disordered over two positions, alternating their concave and convex faces with occupancies of 64% and 36%. The disorder extends to the carboxylate groups, which connect to the corresponding benzophenones in a manner that they themselves are not disordered, as illustrated in Fig. 1.

Nanocrystalline suspensions

Knowing that the determination of an efficient quantum chain must be established by measuring the quantum yield of reaction, which is given by the number of product molecules formed per photon absorbed, we had to verify that samples of **DB-CO$_2$BPh** are able to form nanocrystalline suspensions. It is well known that spectroscopic methods based on measurements of the transmission of light in bulk solids are extremely challenging due to the high optical density, scattering, birefringence, and dichroism that characterize single crystals and polycrystalline samples. These effects also make it difficult to measure the number of photons absorbed by the sample, which is essential for quantum yield measurements. We have previously shown that crystals with sizes that are equal or smaller than the wavelength of light are able to mitigate these optical challenges,[40,41,49,51] making it possible to measure transmission spectra, and to determine quantum yields with particle loadings that are high enough to trap every photon emitted from a calibrated light source. It is now well established that many compounds are able to form aqueous nanocrystalline suspensions of well-defined crystals with average dimensions on the order of 50–500 nm, depending on the specific sample and experimental parameters. In our case, concentrated MeCN solutions of **DB-CO$_2$BPh** were slowly added to a rapidly stirring solution of cetyl trimethyl ammonium bromide (CTAB) at concentrations that are 1/50th of the critical micelle concentration (CMC) in millipore water. Size determination by dynamic light scattering (DLS, ESI page S14†) and scanning electron microscopy revealed prismatic crystals in the range *ca.* 200 nm to *ca.* 1 μm in size (Fig. 2).

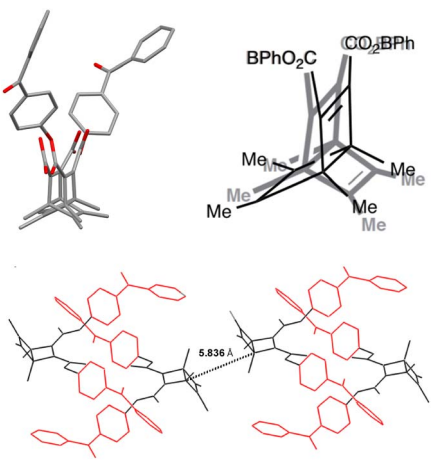

Fig. 1 (Upper left) Capped stick representation of the X-ray molecular structure of DB-CO$_2$BPh illustrating the disorder of the Dewar benzene group and, (upper right) line structure illustrating its two orientations. (Bottom) Packing view illustrating the interdigitated benzophenone arrangement between pairs of molecules, and the closest distance between neighbouring Dewar benzenes, which may be related to the distance for energy transfer.

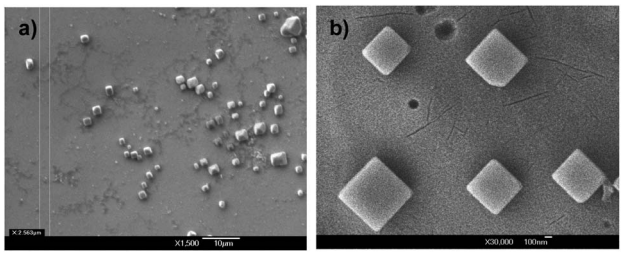

Fig. 2 SEM images of DB-CO_2BPh *ca.* 1 μm size crystals obtained from a dried suspension on a Si surface. Scale bars of (a) 10 micron and (b) 100 nm are shown.

Product analysis in solution and in powder samples

Dilute (*ca.* 0.1 M) degassed acetonitrile solutions of **DB-CO_2H** and **DB-CO_2BPh** exposed to UV light with $\lambda \geq 295$ nm resulted in full conversion to the corresponding Hückel benzenes **HB-CO_2H** and **HB-CO_2BPh** as the only product. Similar results were observed with dry powders placed between two glass slides, indicating that the reaction can proceed as a solid-to-solid transformation. We noticed that reactions of **DB-CO_2BPh** carried out in solution in the presence of oxygen lead to the formation of a new product consistent with the formation of an endoperoxide by reaction of the Dewar benzene with singlet oxygen (Scheme 3).

As expected, reactions carried out with **DB-CO_2BPh** powders and nanocrystalline suspensions were not affected by the presence of oxygen. Samples of **HB-CO_2BPh** could be crystallized and were shown to melt at 142 °C, higher than the melting point of the **DB-CO_2BPh** reactant (*ca.* 109 °C). This suggests the possibility of a solid-to-solid reaction. However, powder X-ray diffraction analysis of samples of **DB-CO_2BPh** before and after reaction revealed that the reaction proceeds by amorphization, rather than a potential single-crystal to single-crystal transformation, or a more common solid-to-solid reaction by a reconstructive phase transition. Unfortunately, we were not able to get diffraction-quality single crystals of the Hückel benzene photoproduct **HB-CO_2BPh**.

Spectroscopic characterization

Included in Fig. 3 is a comparison of the steady state UV spectra of the sensitizer-linked Dewar benzene **DB-CO_2BPh** along with those of samples containing equimolar Dewar benzene methyl ester **DB-CO_2Me**, two equivalents of **4-AcOBPh** that was used as a model chromophore, and a 2 : 1 mixture of **4-AcOBPh** and **DB-CO_2Me**. A relatively weak interaction of the two proximal benzophenone esters and the Dewar benzene can be inferred by noting that the UV spectrum of **DB-CO_2BPh** is more intense and slightly broader than the spectrum obtained when the two

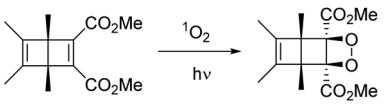

Scheme 3 Reaction of Dewar benzene with singlet oxygen in solution.

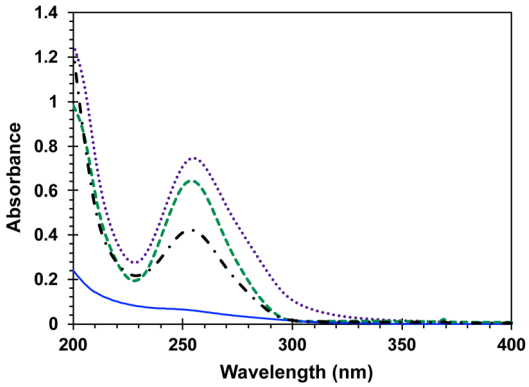

Fig. 3 Steady state UV absorption spectra in MeCN of 2.08 × 10^{-5} M DB-CO_2Me (blue), 4.16 × 10^{-5} M **4-AcOBPh** (green), 1.65 × 10^{-5} M DB-CO_2BPh (purple), and a solution with 1 : 2 molar ratio of the DB-CO_2Me and **4-AcOBPh** (black).

independent chromophores are mixed in the same molar ratio (Fig. 3). From this absorption spectra a ground-state energy value of *ca.* 59 kcal mol^{-1} can be calculated for **DB-CO_2BPh**. We determined the triplet energy of the benzophenone sensitizer by measuring the phosphorescence spectrum of Hückel benzene **HB-CO_2BPh** in dilute 2-methyltetrahydrofuran glass at 77 K (Fig. 4). A characteristic emission with vibrational resolution and a relatively short (4.8 ms) lifetime typical of an n, π* excited state was obtained, along with a triplet energy of *ca.* 65 kcal-mol^{-1} estimated from the onset of the 0–0 vibrational band.

As shown by the green dashed line in Fig. 5, triplet **4-AcOBPh** has the characteristic triplet benzophenone transient absorption with a λ_{max} = 520 nm. Freeze-pump-thawed samples revealed a lifetime of 14.6 μs in dilute MeCN solution (ESI, page S19†). The transient spectrum obtained from solutions of **DB-CO_2BPh** was significantly different with broad absorption bands at *ca.* 480 and 520 nm. The spectrum of **DB-CO_2BPh** can be quenched with oxygen.

Subsequent experiments carried out with Hückel benzene **HB-CO_2BPh** showed that the same transient is formed within

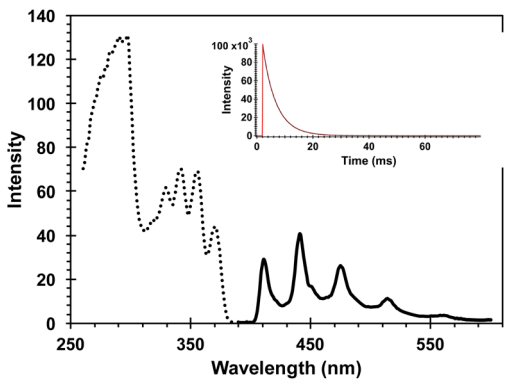

Fig. 4 Phosphorescence excitation (dashed line) and emission (solid line) spectra of HB-CO_2BPh in a 2-methyltetrahydrofuran glass at 77 K. The emission spectrum was detected at 441 nm and the emission obtained by excitation at 343 nm. The phosphorescence decay shown in the inset occurs with a time constant of 4.8 ms.

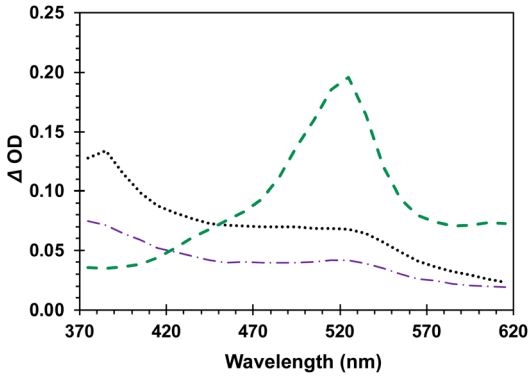

Fig. 5 Transient absorption spectra (λ_{exc} = 355 nm) of 5 mM **4-AcOBPh** (green), 0.76 mM Dewar benzene **DB-CO$_2$BPh** (purple), and 1.5 mM Hückel benzene **HB-CO$_2$BPh** (black) acquired immediately after the laser pulse in Ar saturated MeCN.

the 8 ns pulse, suggesting the spectrum obtained upon irradiation of **DB-CO$_2$BPh** is indeed the triplet state **^{3}HB*-CO$_2$BPh** formed adiabatically from the originally sensitized **^{3}DB*-CO$_2$BPh**, in agreement with steps 1 and 2 in Scheme 2.

Decays measured at 380–420 nm for **DB-CO$_2$BPh** showed clean monoexponential decay (top of Fig. 6) with a lifetime of 503 ns (Table 1). Interestingly, absorption decays for the same sample measured at 530 nm revealed a double exponential with a short-lived component of *ca.* 16 ns that accounts for only 2% of the decay, and a majority (98%) long-lived component of 420 ns. As indicated in Table 1, the decay kinetics obtained from samples of **HB-CO$_2$BPh** were very similar. We tentatively assign the short-lived component at 530 nm as originating from a residual fraction of the originally excited benzophenone-localized triplet states, in the process of transferring their triplet energy to the corresponding Dewar or Hückel benzene chromophore, with the former undergoing a fast adiabatic

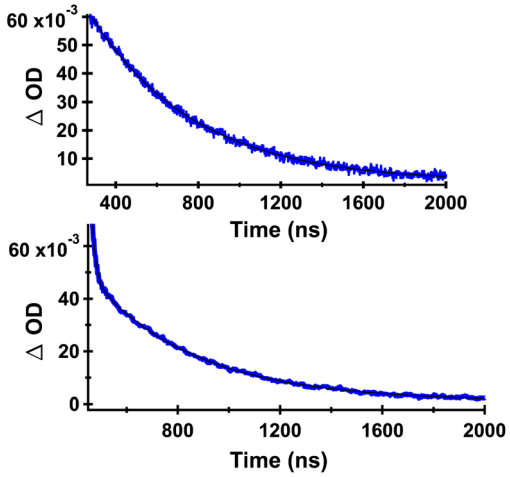

Fig. 6 Decay curves of **DB-CO$_2$BPh** in Ar-saturated MeCN detected at 385 nm (top) and at 530 nm (bottom). Data points are shown in blue and the corresponding fit with a black line. The decay data obtained from **HB-CO$_2$BPh** were essentially identical, indicating that they arise from the same species (Table 1).

Table 1 Transient lifetimes and pre-exponential factors of **DB-CO$_2$BPh** and **HB-CO$_2$BPh** in Ar-saturated MeCN

Compound (λ_{det})[a]	A_1	τ_1 (%w_1)[b,c]	A_2	τ_2 (%w_2)[b,c]	χ^2 (10^4)
DB-CO$_2$BPh (530 nm)	0.024	16.2 (2%)	0.046	420 (98%)	5.7
DB-CO$_2$BPh (385 nm)	—	—	0.058	503	2.2
HB-CO$_2$BPh (530 nm)	0.022	14.5 (2%)	0.14	419 (98%)	11.5
HB-CO$_2$BPh (385 nm)	—	—	1	465	6.5

[a] Detection wavelength in parentheses. [b] Percentage weighted contribution of component "i" is given by $\%w_i = 100\ [(A_i\tau_i)/(A_1\tau_1 + A_2\tau_2)]$. [c] Lifetimes in nanoseconds.

reaction to form the observed triplet Hückel benzene. A monoexponential behavior at the shorter wavelength is consistent with having no significant absorption from the benzophenone chromophore at 385 nm, suggesting that it corresponds to the benzophenone-linked triplet benzene.

The importance of the intramolecular benzophenone sensitizer for the formation of the triplet state chain carrier was also demonstrated with samples of the Dewar benzene methyl ester **DB-CO$_2$Me**, which failed to produce an observable triplet transient on its own, as expected for a fast non-adiabatic singlet-state reaction and a low triplet yield that results from inefficient intersystem crossing. However, the spectroscopic signature of the suggested chain carrier was obtained using the ground-state Hückel benzene methyl ester **HB-CO$_2$Me** as a quencher of triplet **4-AcOBPh**.[47] As shown in Fig. 7, the spectrum of **^{3}4-AcOBPh*** ($E_T \sim 60$ kcal mol^{-1}) evolved into that of **^{3}HB*-CO$_2$Me** as the concentration of the ground-state Hückel benzene increased from 0 mM (Fig. 7, dashed green line) to 100 mM (solid green line). The relatively intense signal of **^{3}4-AcOBPh*** with a maximum at *ca.* 520 nm was replaced by a red-shifted weaker signal with $\lambda_{max} \approx 530$ nm accompanied by an increase of the absorption intensity at 365 nm. Stern–Volmer analysis using changes in the decay rate as a function of increasing quencher concentration (Fig. 7, inset) revealed

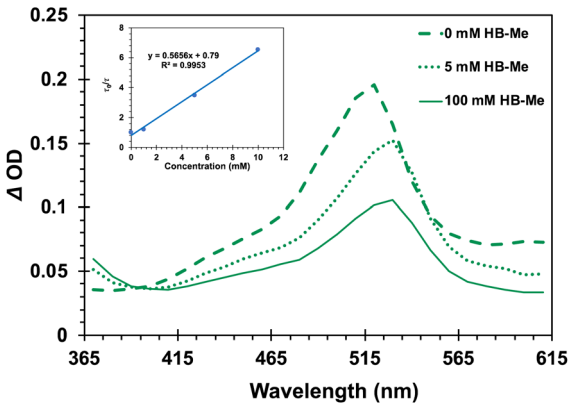

Fig. 7 Evolution of the transient absorption (λ_{exc} = 355 nm) of **4-AcOBPh** as a function of added Hückel benzene **HB-CO$_2$Me** Inset: Stern–Volmer plot built with the lifetime of triplet **4-AcOBPh** in the presence of increasing concentrations of **HB-CO$_2$Me**. A bimolecular rate constant $k_q = 6.3 \times 10^7$ M^{-1} s^{-1} can be estimated from this analysis.

a bimolecular quenching rate constant of $k_q = 6.3 \times 10^7$ M^{-1} s^{-1}, which is about two orders of magnitude slower than diffusion control.[48]

Quantum chain reaction in solution

Knowing that the efficiency of a quantum chain reaction in solution depends on the efficiency of a concentration-dependent energy transfer step, one should expect the observed quantum yield to increase as a function of reactant concentration. With that in mind, we carried out quantum yield determinations with **DB-CO$_2$BPh** concentrations varying from *ca.* 3–50 mM in MeCN. Optically dense, deoxygenated samples of the Dewar benzene and the actinometer **DCK** (Scheme 4) were irradiated in parallel at 312 nm in 5 mL Pyrex tubes to assure that all photons entering each sample were absorbed and all samples were similarly exposed to the light source. The moles of product (N) formed from the sample and the actinometer were calculated with internal standards using ^{1}H NMR.

The following equation was utilized to calculate quantum yields,

$$\Phi_{QC} = \frac{A_{DB\text{-}CO_2BPh}}{A_{DCK}} \times \frac{N_{HB\text{-}CO_2BPh}}{N_{DCK}} \times \frac{\eta_{MeCN}}{\eta_{Benz}} \times \Phi_{DCK}$$

where $A_{DB\text{-}CO_2BPh}$ refers to the absorbance of **DB-CO$_2$BPh**, A_{DCK} is the absorbance of **DCK**, $N_{HB\text{-}CO_2BPh}$ are the number of moles of isomerized product **HB-CO$_2$BPh**, N_{DCK} is the number of moles of reacted **DCK**, and η_{MeCN} and $\eta_{benzene}$ are the refractive indices of MeCN and benzene, respectively. Experiments were run up to five times over different reaction times with conversion values ranging from *ca.* 14% to 75%. Fig. 8 displays the quantum yield of formation of **HB-CO$_2$BPh** photoproduct as a function of the initial concentration of **DB-CO$_2$BPh**, varying from 5 mM to 50 mM. An initial value of $\Phi_{HB\text{-}CO_2BPh} = 2.5 \pm 0.2$ with 5 mM of Dewar benzene increased up to $\Phi_{HB\text{-}CO_2BPh} = 76 \pm 3.5$ with a reactant concentration of 50 mM.

Quantum chain reaction in nanocrystalline suspensions

Aqueous nanocrystalline suspensions of **DB-CO$_2$BPh** and **DCK** were generated by the re-precipitation method.[50] Sample loadings were adjusted to generate optically dense suspensions of **DB-CO$_2$BPh** and **DCK** that were optically matched, as indicated by a UV-Vis immersion probe. Suspensions were irradiated in 3 mL Pyrex tubes at 312 nm. Initial experiments revealed complete conversion of **DB-CO$_2$BPh** at the shortest irradiation time of 10 seconds. A modified setup required suspensions of **DB-CO$_2$BPh** and **DCK** to be irradiated with the former placed behind a 5 × 5 cm neutral density filter with a 1% transmission at 312 nm, so that the photon dose reaching the Dewar benzene

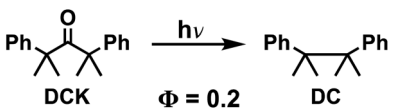

Scheme 4 Photodecarbonylation of DCK in nanocrystalline suspension.

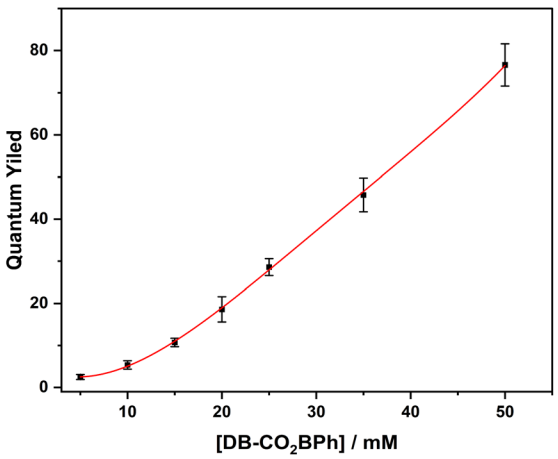

Fig. 8 Quantum yield values of DB-CO$_2$BPh at 5, 10, 15, 20, 25, 35, 50 mM in MeCN solution.

was 100 times weaker (images of the setup can be found in page S25 of the ESI†). The results shown in Fig. 9 reveal that quantum yields of product formation in the suspension sample have values that range from *ca.* $\Phi_{HB\text{-}CO_2BPh} = 90$–$120$, as the extent of reaction increases from 22% to 60% conversion. An increase in the observed quantum yield as a function of accumulated product suggests that the **HB-CO$_2$BPh** product may be a better absorber and potentially a more effective sensitizer. Alternatively, it is also possible that the efficiency of the solid-state adiabatic reaction is improved once the crystals of the reactant are perturbed by the presence of the photoproduct.

While the large reactivity and high quantum yields observed in Fig. 9 support the expectation of an efficient quantum chain reaction, quantum yields on the order of 90–120 are far from the optimum if we assume a radiative triplet-state lifetime on the order of a few milliseconds (Fig. 4, inset) with a fast adiabatic reaction, and exciton hopping in the picosecond time scale. If an adiabatic reaction in the nanosecond time scale were the limiting factor, one should expect chain lengths as high as 10^6, given by the number of reactions that can occur within a few milliseconds. Notably, all our attempts towards the optical

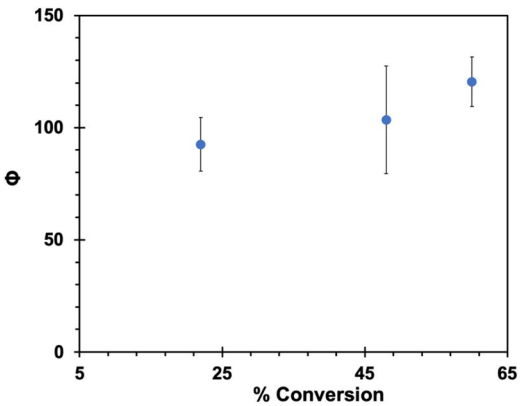

Fig. 9 Quantum yields of formation of HB-CO$_2$BPh in the solid state using suspensions prepared by the re-precipitation method.

detection of the proposed chain carrier ^{3}**HB*-CO$_2$BPh** in the solid state led to no signal detection under conditions where nanocrystals of **4-AcOBPh**, used as a model compound, gave a strong signal with a relatively short 1.2 μs lifetime (ESI, page S18†). The lack of an observable transient suggests that all 90 to 100 reactions in the chain take place within the *ca.* 8 ns laser pulse, indicating that a quenching event must be the chain-limiting factor. In fact, we have previously shown that crystalline benzophenones are susceptible of efficient self-quenching by a reductive charge transfer mechanism.[51] It was shown that nanocrystalline 4,4′-diamino-benzophenone, with strong electron donating aromatic rings ($\sigma^+ = -1.3$), has a triplet lifetime of only *ca.* 6.2 ps at 298 K. On the other end, electron poor 4,4′-benzophenone dicarboxylic acid ($\sigma^+ = 0.42$) has a triplet lifetime of *ca.* 97 μs, which is seven orders of magnitude greater. Self-quenching by the neighboring benzophenones in **HB-CO$_2$BPh** is also evident in solution by comparing the lifetimes of freeze-pump-thawed samples of the former with those of **4-AcOBPh**. A lifetime of 14.6 μs (ESI, page S19†) obtained for the isolated ketone at 298 K in acetonitrile is reduced to 1.9 μs for the bichromophoric compound (ESI, page S20†). This suggests that self-quenching also accounts for the 1.2 μs lifetime of nanocrystalline **4-AcOBPh**, which has a $\sigma^+ = -0.19$ and fits well in the previously published Hammet plot with a reaction constant $\rho = -2.85$.[51]

An alternative explanation based on the quality of the sample was explored by X-ray powder diffraction analysis of centrifuged and dried suspension samples of **DB-CO$_2$BPh**. The results revealed a largely amorphous powder, suggesting that the main sample population in suspension is not crystalline, even though one is able to find crystalline specimens by scanning electron microscopy (Fig. 2). To determine whether the use of a higher quality, more crystalline sample can have a greater effect on the quantum chain, we carried out experiments to compare the extent of reaction between polycrystalline powders suspended in surfactant-containing water, and the nanocrystalline suspensions generated by the re-precipitation method. While aggregate sizes are different, and microcrystals are prone to multiple excitations and triple-triplet annihilation, we reasoned that a greater conversion in suspended polycrystalline powders would qualitatively confirm a greater efficiency for an exciton-mediated quantum chain amplification. Thus, suspended polycrystalline powder samples were prepared by dispensing about 10 mg of **DB-CO$_2$BPh** into 3 mL of a vortexing submiceller CTAB solution; nanocrystalline suspensions generated by the re-precipitation method could be obtained with loading values up to *ca.* 2 mg in 3 mL of submiceller CTAB. While stirring, the two sample types were irradiated using an immersion 302 nm pen lamp. Analyzing the total amount of product generated under such similar conditions revealed that ground crystals suspended in water have quantum yields of $\Phi_{QC} \approx 300$, indicating reactivity that is *ca.* 3–4 times greater than that of the mainly amorphous sample obtained by the re-precipitation method. This result qualitatively confirms that exciton-mediated energy transfer in the crystalline phase has the potential of increasing the quantum amplification in the triplet-sensitized reaction of Dewar benzenes.

Conclusions

Taking advantage of a crystalline tetramethyl Dewar benzene diester with 4-hydroxybenzophenone groups acting as intramolecular triplet sensitizers, we were able to show that triplet quantum chain reactions in the crystalline state display quantum yields of product formation in the range of $\Phi_{QC} = 100$–300, which are greater than those measured as a function of concentration in acetonitrile solution ($\Phi_{QC} = 5$–76), but significantly smaller than those expected based on assumed fast adiabatic reactions, efficient energy transfer, and long triplet lifetimes. The adiabatic and triplet state nature of the valence-bond isomerization reaction was confirmed in solution by taking advantage of laser flash photolysis, where the same transient was observed from both the Dewar and the Hückel benzene isomers. The lack of an observable transient in the solid state was interpreted in terms of a quantum chain that occurs within the *ca.* 8 ns laser pulse, suggesting a quenching mechanism as a limiting factor for the solid state quantum chain. Another contributing factor for the lower than expected quantum chain was unveiled when we showed that samples obtained by re-precipitation are formed as semicrystalline aggregates with coexisting amorphous and crystalline phases. With work in progress, we are addressing the roles of excited-state quenching and crystallinity to find conditions where exciton-mediated reactions can produce quantum chain reactions with values that extend into the thousands or millions of reactions per photon.

Data availability

Data supporting this manuscript is available within the ESI.†

Author contributions

E. Rivera and I. Paul carried out synthesis, photochemical experiments, and nanocrystal characterization. E. Rivera and J. Fajardo, Jr. carried out spectroscopic and kinetic measurements. M. Garcia-Garibay directed this project and all authors contributed to the preparation and revision of the manuscript and have given approval for publication.

Conflicts of interest

There are no conflict of interest to declare.

Acknowledgements

This work was supported by NSF grants CHE-1855342 and CHE-2154210. ER acknowledges the UCLA Graduate Division for a Cota Robles Award and JFJ a UCLA Chancellor's Postdoctoral Fellowship.

Notes and references

1 N. J. Turro, V. Ramamurthy and J. C. Scaiano, *Modern Molecular Photochemistry of Organic Molecules*, U Science, Sausalito, CA, 2010.

2 J. C. Johnson, A. J. Nozik and J. Michl, Triplet Yield from Singlet Fission in a Thin Film of 1,3-Diphenylisobenzofuran, *J. Am. Chem. Soc.*, 2010, **132**, 16302–16303.
3 S. Jin, H.-J. Son, O. K. Farha, G. P. Wiederrecht and J. T. Hupp, Energy Transfer from Quantum Dots to Metal-Organic Frameworks for Enhances Light Harvesting, *J. Am. Chem. Soc.*, 2013, **135**, 955–958.
4 M. K. Manna, S. Shokri, G. P. Wiederrecht, D. J. Gosztola and A. J. Ayitou, New perspectives for triplet-triplet annihilation-based photon upconversion using all-organic energy donor & acceptor chromophores, *Chem. Commun.*, 2018, **54**, 5809–5818.
5 D. N. Congreve, J. Lee, N. J. Thompson, E. Hontz, S. R. Yost, P. D. Reusswig, M. E. Bahlke, S. Reineke, V. Voorhis and M. A. Baldo, External quantum efficiency above 100% in a singlet-exciton-fission-based organic photovoltaic cell, *Science*, 2013, **340**, 334–337.
6 M. F. Joubert, Photon avalanche upconversion in rare earth laser materials, *Opt. Mater.*, 1999, **11**, 181–203.
7 J. C. Scaiano, L. J. Johnston, W. G. McGimpsey and D. Weir, Photochemistry of organic reaction intermediates: novel reaction paths induced by two-photon laser excitation, *Acc. Chem. Res.*, 1988, **21**, 22–29.
8 T. N. Singh-Rachford and F. N. Castellano, Photon upconversion based on sensitized triplet–triplet annihilation, *Coord. Chem. Rev.*, 2010, **254**, 2560–2573.
9 K. Miyata, F. S. Conrad-Burton, F. L. Geyer and X.-Y. Zhu, Triplet Pair States in Singlet Fission, *Chem. Rev.*, 2019, **119**, 4261–4292.
10 M. B. Smith and J. Michl, Singlet Fission, *Chem. Rev.*, 2010, **110**, 6891–6936.
11 H. L. Hyndman, B. M. Monroe and G. S. Hammond, Mechanisms of photochemical reactions in solution. LX. Photochemical isomerization of 2,4-hexadiene via a quantum-chain mechanism", *J. Am. Chem. Soc.*, 1969, **91**, 2852–2859.
12 N. J. Turro, J. Mcvey, V. Ramamurthy and P. Lechtken, Adiabatic Photoreactions of Organic Molecules, *Angew. Chem., Int. Ed. Engl.*, 1979, **18**, 572–586.
13 T. Forster, Diabatic and Adiabatic Processes in Photochemistry, *Pure Appl. Chem.*, 1970, **24**, 443–449.
14 T. Forster, Excimers, *Angew. Chem., Int. Ed. Engl.*, 1969, **8**, 333.
15 N. J. Turro, P. Lechtken, A. Lyons, R. R. Hautala, E. Carnahan and T. J. Katz, Molecular photochemistry. LXIV. Photochemical generation of electronically excited organic products in adiabatic pericyclic photoreactions. Unexpected propensity toward spin inversion in a retrocycloaddition and in a valence isomerization, *J. Am. Chem. Soc.*, 1973, **95**, 2035–2037.
16 J. Saltiel, D. E. Townsend and A. Sykes, Quantum chain process in the sensitized cis-trans photoisomerization of 1,3 dienes, *J. Am. Chem. Soc.*, 1973, **95**, 5968–5973.
17 J. Saltiel, J. D'Agostino, E. D. Megarity, L. Metts, K. R. Neuberger, M. Wrighton and O. C. Zafiriou, The cis-trans photoisomerization of olefins, *Org. Photochem.*, 1973, **3**, 1–113.
18 W. A. Yee, S. J. Hug and D. S. Kliger, Direct and sensitized photoisomerization of 1,4-diphenylbutadienes, *J. Am. Chem. Soc.*, 1988, **110**, 2164–2169.
19 S. Ganapathy and R. S. H. Liu, Photoisomerization of polyenes. 30. Quantum chain processes in photoisomerization of the all-trans, 7-cis, and 11-cis isomers of retinal, *J. Am. Chem. Soc.*, 1992, **114**, 3459–3464.
20 M. Sundahl and O. Wennerstrom, Catalysis of a photochemical reaction; a cis-trans isomerization proceeding by a quantum chain process, *J. Photochem. Photobiol., A*, 1996, **98**, 117–120.
21 M. Brink, H. Jonson and M. Sundahl, Catalysis of triplet state cis-trans isomerizations making a quantum chain process more efficient, *J. Photochem. Photobiol., A*, 1998, **112**, 149–153.
22 D. G. Whitten and J. A. Mercer-Smith, Photosensitization o Stilbene Isomerization by Palladium and Platinum Porphyrins, an Intermolecular Quantum Chain Process, *J. Am. Chem. Soc.*, 1978, **110**, 2620–2625.
23 V. R. Gopal, M. A. Reddy and V. J. Rao, Wavelength Dependent Trans to Cis and Quantum Chain Isomerizations of Anthrylethylene Derivatives, *J. Org. Chem.*, 1995, **60**, 7966–7973.
24 J. Saltiel, S. Wang, D. Ko and D. A. Gormin, Cis-Trans Photoisomerization of the 1,6-Diphenyl-1,3,5-hexatrienes in the Triplet State. The Quantum Chain Mechanism and the Structure of the Triplet State, *J. Phys. Chem. A*, 1998, **102**, 5383–5392.
25 K. Tokumaru and T. Arai, Factors Determining the Adiabatic or the Diabatic Pathway of the Photoisomerization of Unsaturated Bonds, *Bull. Chem. Soc. Jpn.*, 1995, **68**, 1065–1087.
26 V. P. Kazakov, A. I. Voloshin and N. M. Shavaleev, Chemiluminescence in visible and infrared spectral regions and quantum chain reactions upon thermal and photochemical decomposition of adamantylideneadamantane-1,2-dioxetane in the presence of chelates $Pr(dpm)_3$ and $Pr(fod)_3$, *J. Photochem. Photobiol.*, 1998, **11**, 177–186.
27 P. Lechtken, A. Yekta and N. J. Turro, Tetramethyl-1,2-dioxetane. Mechanism for an autocatalytic decomposition. Evidence for a quantum chain reaction, *J. Am. Chem. Soc.*, 1973, **95**, 3027–3028.
28 N. J. Turro, N. E. Schore and A. Yekta, Quantum chain processes. Novel procedure for measurement of quenching parameters. Evidence that exothermic triplet-triplet energy transfer is not diffusion limited and an estimation of the efficiency of exothermic quenching in a solvent cage, *J. Am. Chem. Soc.*, 1974, **96**, 1936–1938.
29 N. J. Turro and W. H. Waddell, Quantum chain processes. Direct observation of high quantum yields in the direct and photosensitized excitation of tetramethyl-1,2-dioxetane, *Tetrahedron Lett.*, 1975, **25**, 2069–2072.
30 G. B. Schuster, N. J. Turro, H. Steinmetzer, A. P. Schaap, G. Faler, W. Adam and J. C. Liu, Adamantylideneadamantane-1,2-dioxetane. Chemiluminescence and decomposition kinetics of an

unusually stable 1,2-dioxetane, *J. Am. Chem. Soc.*, 1975, **97**, 7110–7117.

31 T. Wilson and A. P. Schaap, Chemiluminescence from cis-diethoxy-1,2-dioxetane. Unexpected effect of oxygen, *J. Am. Chem. Soc.*, 1971, **93**, 4126–4136.

32 N. J. Turro, P. Lechtken, N. E. Schore, G. Schuster, H. Steinmetzer and A. Yekta, Tetramethyl-1,2-dioxetane. Experiments in chemiexcitation, chemiluminescence, photochemistry, chemical dynamics, and spectroscopy, *Acc. Chem. Res.*, 1974, **7**, 97–105.

33 R. V. Carr, B. Kim, J. K. McVey, N. C. Yang, W. Gerhartz and J. Michl, Photochemistry and photophysics of 1,4-dewarnaphthalene, *Chem. Phys. Lett.*, 1976, **39**, 57–60.

34 N. C. Yang, R. V. Carr, E. Li, J. K. McVey and S. A. Rice, 2,3-Naphtho-2,5-bicyclo[2.2.0]hexadiene, *J. Am. Chem. Soc.*, 1976, **96**, 2297–2298.

35 G. Kuzmanich, A. Natarajan, K. K. Chin, M. Veerman, C. J. Mortko and M. A. Garcia-Garibay, Solid-state photodecarbonylation of diphenylcyclopropenone: a quantum chain process made possible by ultrafast energy transfer, *J. Am. Chem. Soc.*, 2008, **130**, 1140–1141.

36 G. Kuzmanich, M. N. Gard and M. A. Garcia-Garibay, Photonic amplification by a singlet state quantum chain reaction in the photodecarbonylation of crystalline diarylcyclopropenones, *J. Am. Chem. Soc.*, 2009, **131**, 11606–11614.

37 R. C. Powel and A. G. Soos, Singlet exciton energy transfer in organic solids, *J. Lumin.*, 1975, **11**, 1–45.

38 C. E. Swenberg and N. E. Gaecintov, in *Organic Molecular Photophysics*, ed. J. B. Birks, John Wiley and Sons, London, 1973, vol. 1.

39 Z. S. Yoon, M.-C. Yoon and D. Kim, Excitonic Coupling in covalently linked multiporphyrin systems by matrix diagonalization, *J. Photochem. Photobiol., C*, 2005, **6**, 249–263.

40 C. Swenberg and M. Pope, *Electronic Processes in Organic Crystals and Polymers*, Oxford University Press, 1999.

41 Z. Soos and R. Powell, Generalized Random-Walk Model for Singlet-Exciton Energy Transfer, *Phys. Rev. B: Solid State*, 1972, **6**, 4035–4046.

42 S. C. Doan, G. Kuzmanich, M. N. Gard, M. A. Garcia-Garibay and B. J. Schwartz, Ultrafast spectroscopic observation of a quantum chain reaction: The photodecarbonylation of nanocrystalline diphenylcyclopropenone, *J. Phys. Chem. Lett.*, 2012, **3**, 81–86.

43 A. Ryasnyanskiy and I. Biaggio, Triplet exciton dynamics in rubrene single crystals, *Phys. Rev. B: Condens. Matter Mater. Phys.*, 2011, **84**, 193203.

44 N. J. Turro, V. Ramamurthy and T. J. Katz, Energy Storage and Release. Direct and sensitized photoreactions of Dewar benzene and prismane, *Nouv. J. Chim.*, 1978, **1**, 363–365.

45 P. B. Merkel, Y. Roh, J. P. Dinnocenzo, D. R. Robello and S. Farid, Highly Efficient Triplet Chain Isomerization of Dewar Benzenes: Adiabatic Rate Constants from Cage Kinetics, *J. Phys. Chem. A*, 2007, **111**, 1188–1199.

46 L. Ferrar, M. Mis, J. P. Dinnocenzo, S. Farid, P. B. Merkel and D. R. Robello, Quantum Amplified Isomerization in Polymers Based on Triplet Chain Reactions, *J. Org. Chem.*, 2008, **73**, 5683–5692.

47 M. Tomasulo, S. L. Kaanumal, S. Sortino and F. M. Raymo, Synthesis and Properties of Benzophenone–Spiropyran and Naphthalene–Spiropyran Conjugates, *J. Org. Chem.*, 2007, **72**, 595–605.

48 The bimolecular diffusion rate constant in acetonitrile is 6.83×10^9 M^{-1} s^{-1}, *CRC Handbook of Chemistry and Physics*, ed. R. C. Weast, CRC Press, Inc., Boca Raton, FL, 68th edn, 1987–1988.

49 M. Veerman, M. J. E. Resendiz and M. A. Garcia-Garibay, Large Scale Photochemical Reactions of Nanocrystalline suspensions: A Promising Green Chemistry Method, *Org. Lett.*, 2006, **8**, 2615–2617.

50 H. Kasai, H. S. Nalwa, H. Oikawa, S. Okada, H. Matsuda, N. Minami, A. Kakuta, K. Ono, A. Mukoh and H. Nakanishi, A Novel Preparation Method of Organic Microcrystals, *Jpn. J. Appl. Phys.*, 1992, **31**, L1132–L1134.

51 G. Kuzmanich, S. Simoncelli, M. N. Gard, F. Spanig, B. L. Henderson, D. M. Guldi and M. A. Garcia-Garibay, Excited State Kinetics in Crystalline Solids: Self-Quenching in Nanocrystals of 4,4'-Disubstituted Benzophenone Triplets Occurs by a Reductive Quenching Mechanism, *J. Am. Chem. Soc.*, 2011, **43**, 17296–17306.